ENERGY BALANCE IN SINGLE EXPOSURE MULTISPECTRAL SENSORS

Hugues Péguillet, Jean-Baptiste Thomas, Pierre Gouton

University of Bourgogne
LE2I
Dijon, France

Yassine Ruichek

IRTES-SET,
UTBM
90010 Belfort cedex, France

ABSTRACT

Recent simulations of multispectral sensors are based on a simple Gaussian model, which includes filters transmittance and substrate absorption. In this paper we want to make the distinction between these two layers. We discuss the balance of energy by channel in multispectral solid state sensors and propose an updated simple Gaussian model to simulate multispectral sensors. Results are based on simulation of typical sensor configurations.

Index Terms— Spectral and color filter arrays, light sensor, transmittance filters, energy balance.

1. INTRODUCTION

In recent works on multispectral acquisition, energy balance of the sensor is not taken into account clearly into the model. Most simulations consider filters with a Gaussian shape [20, 18, 17] leads to no distinction between the interference filters and the substrate. Filters can be metallic filters [16, 5, 19, 11, 2, 21] or nano structure filters [14, 6, 9], and the substrate is often silicon or doped silicones [7][8], germanium, AsGa, indium, etc. We propose to study how different spectral configurations would impact the quality of acquisition of a sensor. We focus typically on solid state sensors based on CFA (Color Filter Array) [15, 1] technology, such as Bayer configuration [4] or SFA (Spectral Filters Array) technology [13, 12, 20], since there is no real mean of having a different acquisition time by channel on such sensors. We propose an extended Gaussian model of filters, which guarantee the energy balance of the sensor by optimizing the standard deviation or the amplitude of the filter in addition to a given substrate and a typical, standard or neutral illumination.

Let us recall that the energy E is a function of the number of wave, i.e. function of the wavelength:

$$E_{ph} = h\nu = \frac{hc}{\lambda} \tag{1}$$

where h is the Plank constant ($6.626 * 10^{34}$J.s), c is the speed of light, and λ is the wavelength. In this paper λ is considered to be between 300 and 1100 nm.

If we replace the constants by their value, the photon energy is expressed in electron-volts ($1eV = 1.602.10^{-19}$J) and if the wavelength is expressed in nanometers, we have:

$$E_{ph}[eV] = \frac{1240}{\lambda[nm]} \tag{2}$$

Thus, low wavelengths contain more energy than higher ones. The definition of a multispectral sensor should carefully take this fact into account.

Indeed, one channel might be over-exposed (saturated), while another might be under-exposed (noise level). Thus it appears that some balancing shall be performed in order to optimize the shape of the transmittance filters. While the number of filter increases, and their bandwidth decreases, this becomes a critical issue.

We recall the usual model of camera acquisition and add a term to consider each wavelength energy. From this model, we propose a constraint that should guarantee the energy balance of the senor, and a simple integration model for future simulations. This is illustrated with results from simulation of typical sensor configurations.

2. ENERGY BALANCING

2.1. Model

Let us consider $L(\lambda)$ the radiance of the scene, resulting of the convolution of the illumination $I(\lambda)$ and the object reflectance $R(\lambda)$, the transmittance of a filter $T(\lambda)$ and the sensitivity of the substrate to energy $s(\lambda)$; $z^{(k)}$ is the given value of the sensor for $L(\lambda)$ and a channel k. Usually, $k \in \{R, V, B\}$ for a CFA configuration, $k \in \{F_1, ..., F_n\}$ for an SFA multispectral configuration with N channels.

Considering a typical camera model [3], substrate, energy and filters are mixed up in $G^{(k)}(\lambda)$:

$$\rho^{(k)} = F^{(k)}(z^{(k)}) = \int_{\Lambda} L(\lambda)G^{(k)}(\lambda)d\lambda \tag{3}$$

where $F^{(k)}$ is a linearization function, and $\rho^{(k)}$ the actual linear response of the camera. $F^{(k)}$ can be typically a *gamma* correction and includes the camera *offset*.

If we wish to include the energy of every wavelength within this equation, we simply need to weight the quantity of equation 3 by the energy estimation:

$$\rho^{(k)} = hc \int_{\Lambda} L(\lambda) T^{(k)}(\lambda) s^{(k)}(\lambda) \frac{d\lambda}{\lambda} \tag{4}$$

In order to simplify the equation, and considering that the absorption of silicon as given as curves includes the energy in the following of this paper, we consider:

$$S(\lambda) = \frac{hc}{\lambda} s(\lambda) \tag{5}$$

Thus, Equation 4 becomes:

$$\rho^{(k)} = \int_{\Lambda} L(\lambda) T^{(k)}(\lambda) S^{(k)}(\lambda) d\lambda \tag{6}$$

If the camera contains N different channels k ($k \in [1...N]$, we have energy balance when and only when,

$$\begin{array}{l} \forall \lambda \in [300, 1100] \\ \forall k, k \in N, hc \int_{\Lambda} I(\lambda) R_W(\lambda) T(\lambda) s(\lambda) \frac{d\lambda}{\lambda} = A \end{array} \tag{7}$$

where F_k is the spectral transmittance of channel k, A is constant $\forall\ R_W(\lambda)$. $R_W(\lambda)$ is a flat reflectance object.

In a more compact notations, for a *white*[1] radiance $L_W(\lambda)$, we have:

$$\forall k, k \in [1...N], \int_{\Lambda} L_W(\lambda) T^{(k)}(\lambda) S(\lambda) d\lambda = A \tag{8}$$

In the following, we use this model to evaluate different sensor configurations and optimize the transmittance $k(\lambda)$ of the filters.

2.2. Simulations

In this section, we use the model above to illustrate the importance of filters.

2.2.1. Discrete model definition

We will consider the reflectance $R(\lambda)$ of the scene as perfectly uniform through wavelengths ($R_W(\lambda)$). In our preliminary results we consider $I(\lambda)$ as a flat illumination. Thus, $L(\lambda)$ is a flat radiance in the following, i.e. a vector of one that can be removed from the discrete representation of the above model.

With these assumptions, a discrete version of Equation 3 becomes:

[1]White radiance means here a given illumination and a flat reflectance object. This implies basically that the camera would be naturally white balanced for this given illumination

$$\rho^{(k)} = \mathbf{T}.\mathbf{S}' \tag{9}$$

where . represents the inner product between vector $\mathbf{T}$ and the transpose of $\mathbf{S}$. $\mathbf{T}$ is a vector containing the transmittance properties of each filter. $\mathbf{S}$ is a vector containing the absorption of silicon. Then, our filters are optimized when $\rho^{(k)} = A$ for each k. A is a given value, which might depends on acquisition time, intensity of lighting, etc.

2.2.2. Consideration on Silicon

This simulation demonstrates the importance of energy balance in the sensor.

For this simulation, we consider the case of a silicon substrate. A similar process can be used for any substrate for which absorption by wavelength is known. Photons with an energy bellow $1.1eV$ will go through silicon without interaction[7]. This corresponds, by relation (2), to a theoretical wavelength larger than $1125nm$. The structure of the sensor will, in fact, cut this limit sooner than the theoretical limit. [7].

This simulation does not include the optical effects. Indeed, the layer of silicon can act as a Fabry-Pérot interferometer[10], i.e. , which modifies the absorption properties of the substrate.

Without the optical effects, we can use the absorption properties of silicon as defined in Fig.1, based on data from the technical report of Darmont [7].

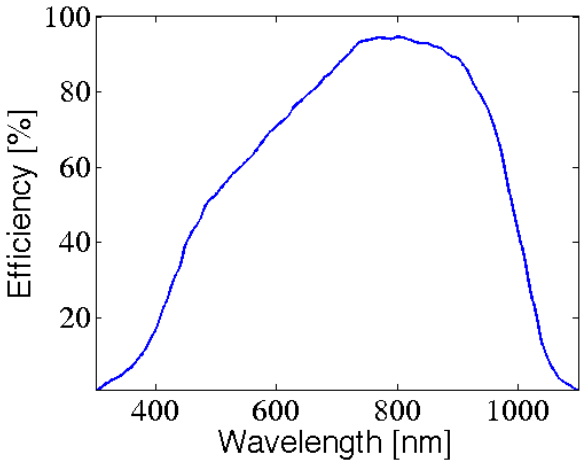

Fig. 1. Silicon efficiency in function of wavelength. This curve is based on Darmont's technical report [7] and ignores optical effects. We observe that the silicon efficiency is not linear.

To start with, we consider the case of a camera based on similar Gaussian filters. Three cases are investigated: 3 filters, 5 filters, and 10 filters. Ten filters are represented with the silicon efficiency in background on Figure 2. The results of

the convolution, following the discrete model are shown in Table 1. Results are normalized by dividing the value by the number of samples.

These results show that the difference of values might be ten times larger from one filter to another with 10 different filters. Differences are less important in a 3 filters configuration (up to 2).

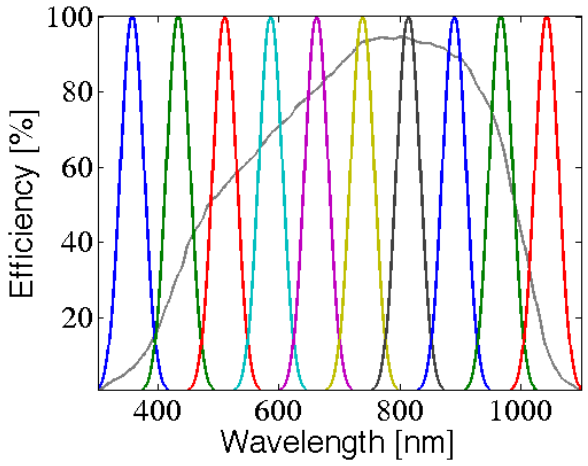

Fig. 2. Ten generated filters in function of wavelength with silicon efficiency in background. The light is not taken into account.

3. FILTER OPTIMIZATION

We use this model to derive an optimization process that allows building a filter set, while taking into account some parameters, such as the substrate absorption and the spectral properties of the illumination. Given an arbitrary value A, we propose to optimize the filters by modifying the properties of the Gaussian for each channel, following Equation 8, in order to have energy balance. Given the equation of the normal Gaussian law:

$$f(x) = B\frac{1}{\sigma\sqrt{2\pi}}\exp -\frac{1}{2}(\frac{x-\mu}{\sigma})^2 \qquad (10)$$

we identify μ as the bandpass peak of the filter at one wavelength, σ as indicator of the width of the filter and B, a real constant value below 1 as the amplitude of the filter. We propose to optimize the parameters σ and B in order to reach the energy balance in some given conditions. In the following, we optimize each parameter independently.

3.1. Energy balancing by changing the amplitude

In order to calculate the value of B for which the filters are balanced, we used a rescale algorithm. We first calculate the convolution with the uncorrected filters. Then, we consider the greatest value of the convolution. We normalize the values by dividing the greatest value by the convolution of each filter. We apply a second normalization to obtain some values between 0 and 1, which correspond to $B_1, B_2 ... \ B_N$. Then, we multiply each filter by its scaling factor $B_1, B_2 ... \ B_N$.

We implemented our algorithm to change the magnitude B of the Gaussian and obtain energetically balanced filters (Figure 3, Figure 4 and Figure 5). The value of σ is constant during the process and is equal to 57.1 for three filters, 36.36 for five filters and 19.04 for ten filters.

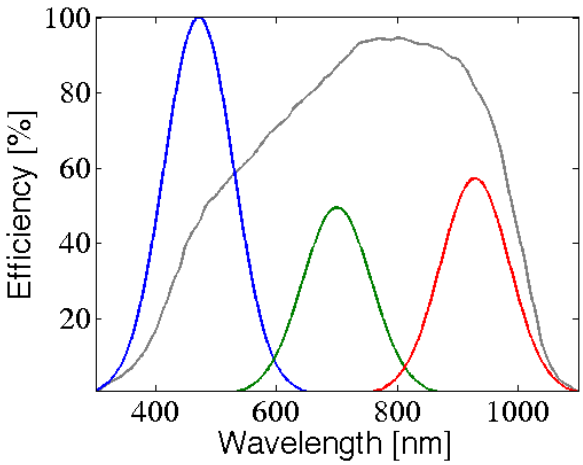

Fig. 3. Three amplitude corrected filters in function of wavelength with silicon efficiency in background. We observe that the amplitude of each filter depends on the response of silicon

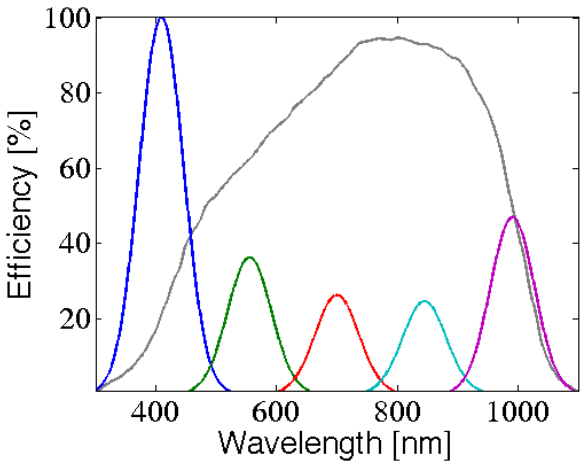

Fig. 4. Five amplitude corrected filters in function of wavelength with silicon efficiency in background. The amplitude of each filter depends on the response of silicon.

These figures include the fact that the energy of the low wavelength is higher than the high wavelength, and the silicon

Filter	F_1^{10}	F_2^{10}	F_3^{10}	F_4^{10}	F_5^{10}	F_6^{10}	F_7^{10}	F_8^{10}	F_9^{10}	F_{10}^{10}
ρ	43,45	187,47	326,12	407,3	481,57	549,8	559,66	531,67	388,57	87,63
Filter	F_1^5	F_2^5	F_3^5	F_4^5	F_5^5					
ρ	259,04	713,39	985,37	1049,19	550,88					
Filter	F_1^3	F_2^3	F_3^3							
ρ	759,05	1535,58	1323,35							

Table 1. Values of the convolution ρ depending on the filter for 3, 5, and 10 filters.

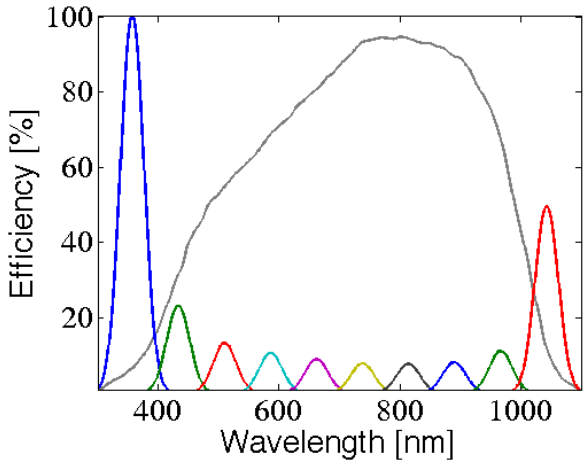

Fig. 5. Ten amplitude corrected filters in function of wavelength with silicon efficiency in background. In that case the lowest amplitude of most of the corrected filters is really low.

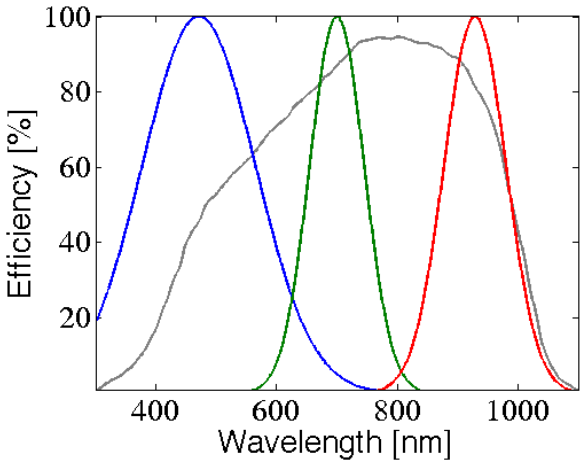

Fig. 6. Three bandwidth corrected filters in function of wavelength with silicon efficiency in background. The bandwidth is larger when the silicon efficiency is lower.

response is not uniform.

We can observe that the difference between filters increases as the bandwidth of the filters become narrow.

In figure 5 we can see that we severely reduced the transmittance efficiency of most of the filters. This appears to be an inefficient situation for practical implementation, considering the noise that might appear.

3.2. Energy balancing by changing the standard deviation

The aim is to obtain the same convolution A for N filters. In the presented results, we use $A = \frac{A^{(1)}.....A^{(N)}}{N}$

We calculate the convolution depending on the σ parameter of the Gaussian: $f(\sigma) = \hat{A}$

The result must be equal to A. In order to obtain the value of σ for which the filter has the value A, we search for the minimum of the function $f'(\sigma) = |A - \hat{A}|$

The value of σ for which the convolution is equal to A allows us to generate the balanced Gaussian filters. The obtained energetically ballanced filters are presented in Figure 6, Figure 7 and Figure 8.

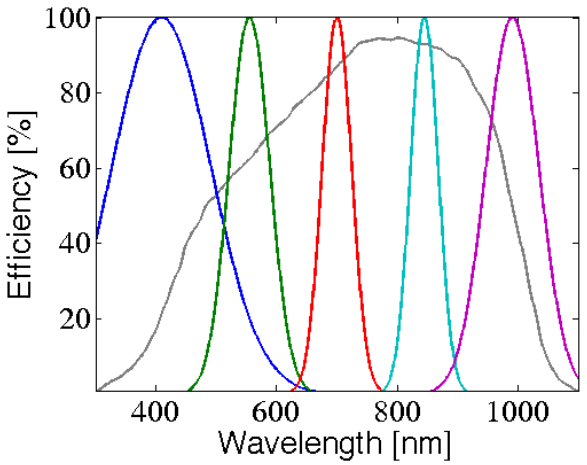

Fig. 7. Five bandwidth corrected filters in function of wavelength with silicon efficiency in background.

4. A CONCRETE CASE: D65 ILLUMINANT AND VISIBLE SPECTRAL RESPONSE ON A FIVE FILTERS SFA CAMERA

We consider now a practical case with a camera consisting of an SFA of five filters distributed over the visible spec-

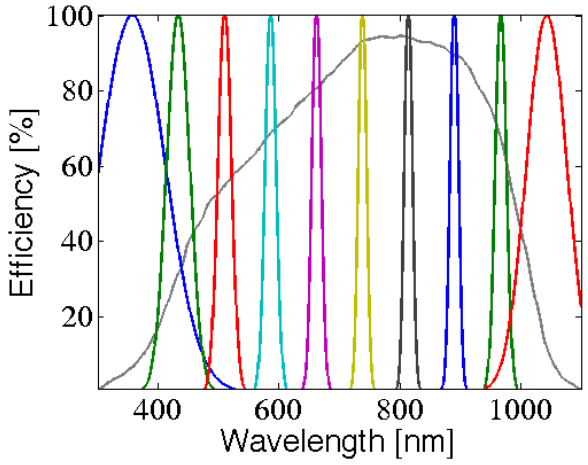

Fig. 8. Ten bandwidth corrected filters in function of wavelength with silicon efficiency in background. We observe some gaps and overlapping, which must be corrected.

tral range, shooting a scene illuminated by a D65 illuminant. Equation 8 becomes Equation 11 in discrete terms.

$$\sum \mathbf{L_{D65}}.\mathbf{T}.\mathbf{S} \tag{11}$$

We consider a range of [300, 780]nm.

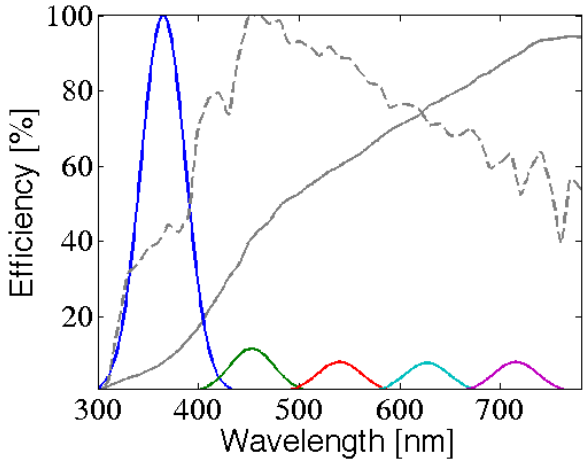

Fig. 9. Spectral response of the silicon (plain gray line), normalized illuminant D65 (dashed gray line) with 5 filters optimized in amplitude.

The optimization shows that while optimizing the amplitude of the filter, we have an important reduction of energy. Indeed, 90% of the energy should be filtered to guarantee the balance. This result is illustrated in Figure 9 and is similar to the results shown in Figure 5. Similar results are observed when we perform the optimization on sigma, which suggests again that we need to add constraints to this optimization to reach a practical sensor configuration.

The optimization shows that while we optimize the amplitude of the filter, we have an important reduction of energy, around 10%. This is similar to the results shown in Figure 5. Similar results are observed when we perform the optimization on sigma. This suggest that we need to add constraints to this optimization.

5. CONCLUSION

We proposed to optimize the energy of each filters in an SFA camera configuration. Results show that the loss of energy induced by such a process is critical and is not acceptable in most sensor configurations. Moreover, when we optimized the band pass of the filter (sigma parameter), we observe some gaps in the spectra or too much overlapping (Figure 8).

This suggests that further works would focus on combining amplitude and bandwidth into a single optimization function $f(B, \sigma)$ under constraints. The set of constraints might include:

1. There should be no gap in the spectral domain, otherwise some spectral information will be lost for some wavelengths.
2. There should be no full overlapping of a filter over another.
3. Peak attenuation should not be so large. A good compromise must be found.
4. A value should be optimized regarding to these parameters. We arbitrarily used A = A(1).....(N)=N but a value that fits better the previous parameters could be found.

Energy balance is one of the problems to address for this technology, but other problems need to be solved by further works, including blurr from chromatic aberration.

6. ACKNOWLEDGEMENTS

Thanks to the regional council of Franche-Comté for cofunding this work.

7. REFERENCES

[1] David Alleysson, Sabine Susstrunk, and Jeanny Hérault. Linear demosaicing inspired by the human visual system. *Image Processing, IEEE Transactions on*, 14(4):439–449, 2005.

[2] Joseph H. Apfel. Infra-red interference filter, 1972. US Patent 3,682,528.

[3] Kobus Barnard and Brian Funt. Camera characterization for color research. *Color Research & Application*, 27(3):152–163, 2002.

[4] Bryce E. Bayer. Color imaging array, 1976. US Patent 3,971,065.

[5] S Belgacem and R Bennaceur. Propriétés optiques des couches minces de sno2 et cuins2 airless spray. *Revue de Physique Appliquée*, 25(12):1245–1258, 1990.

[6] Yajie Chen, Guohui Tian, Kai Pan, Chungui Tian, Juan Zhou, Wei Zhou, Zhiyu Ren, and Honggang Fu. In situ controlled growth of well-dispersed gold nanoparticles in TiO2 nanotube arrays as recyclable substrates for surface-enhanced raman scattering. *Dalton Transactions*, 41(3):1020–1026, 2012.

[7] Arnaud Darmont. Spectral response of silicon image sensors. Technical report, Aphesa, April 2009. White paper.

[8] Eric R Fossum. Cmos image sensors: Electronic camera-on-a-chip. *Electron Devices, IEEE Transactions on*, 44(10):1689–1698, 1997.

[9] Yoshiaki Kanamori, Masaya Shimono, and Kazuhiro Hane. Fabrication of transmission color filters using silicon subwavelength gratings on quartz substrates. *Photonics Technology Letters, IEEE*, 18(20):2126–2128, 2006.

[10] Wenjie Liang, Marc Bockrath, Dolores Bozovic, Jason H Hafner, M Tinkham, and Hongkun Park. Fabry-perot interference in a nanotube electron waveguide. *Nature*, 411(6838):665–669, 2001.

[11] M.A. Mahdi, S.J. Kasem, J.J. Hassen, A.A. Swadi, and S. K. J. A l Ani. Structural and optical properties of chemical deposition cds thin films. *International Journal of Nanoelectronics and Materials*, vol.2:163–172, 2009.

[12] Lidan Miao and Hairong Qi. The design and evaluation of a generic method for generating mosaicked multispectral filter arrays. *IEEE Trans. Image Processing*, 15(9):2780–2791, August 2006.

[13] Lidan Miao, Hairong Qi, and Wesley E. Snyder. A generic binary tree-based progressive demosaicking method for multispectral filter array. In *Image Processing, IEEE Transactions on*, pages 3221 –3224, October 2006.

[14] Nghia Nguyen-Huu, Yu-Lung Lo, Yu-Bin Chen, and Tsai-Yu Yang. Subwavelength metallic gratings as an integrated device: polarized color filter. In *Proceedings of SPIE*, volume 7934, page 79340U, 2011.

[15] Laurel J Pace and Jeffrey C Blood. Color filter arrays, August 16 1988. US Patent 4,764,670.

[16] Pierre Rouard. Sur les propriétés optiques des lames minces de platine et leur comparaison avec celles d'autres métaux. *Le journal de physique et le radium*, 11(7):390–393, 1950.

[17] Zahra Sadeghipoor, Yue M Lu, and Sabine Süsstrunk. Optimum spectral sensitivity functions for single sensor color imaging. In *Society of Photo-Optical Instrumentation Engineers (SPIE) Conference Series*, volume 8299, page 3, 2012.

[18] Raju Shrestha, Jon Y. Hardeberg, and Rahat Khan. Spatial arrangement of color filter array for multispectral image acquisition. In *Proceedings of SPIE;7875*. Society of Photo Optical Instrumentation Engineers (SPIE), 2011.

[19] Jesus M Siqueiros, Luis E Regalado, and Roberto Machorro. Determination of (n, k) for absorbing thin films using reflectance measurements. *Applied optics*, 27(20):4260–4264, 1988.

[20] Xingbo Wang, Jean-Baptiste Thomas, Jon Y Hardeberg, and Pierre Gouton. Median filtering in multispectral filter array demosaicking. In *IS&T/SPIE Electronic Imaging*, pages 86600E–86600E. International Society for Optics and Photonics, 2013.

[21] Yu Wang. Low-cost thin-metal-film interference filters, February 29 2000. US Patent 6,031,653.